Cell Proliferation

Cell Prolif., 2010, **43**, 562–572 doi: 10.1111/j.1365-2184.2010.00705.x

Assessment of cell proliferation and muscular structure following surgical tongue volume reduction in pigs

W. Ye*,†, A. F. Abu* and Z. J. Liu*

**Department of Orthodontics, University of Washington, Seattle, WA, USA and †Department of Orthodontics, Fourth Military Medical University, Xi'an, China*

Received 4 *February* 2010; *revision accepted* 22 *April* 2010

Abstract

Objectives: Tongue volume reduction is an adjunct treatment in several orofacial orthopaedic procedures for various craniofacial deformities; it may affect structural reconstitution and functional recovery as a result of the repair process. The aim of this study was to investigate myogenic regeneration and structural alteration of the tongue following surgical tongue volume reduction.

Materials and methods: Five 12-week-old sibling pairs of Yucatan minipigs (three males and two females) were used. Midline uniform glossectomy was performed on one of each pair (reduction); siblings had identical incisions without tissue removal (sham). All pigs were raised for a further 4 weeks and received 5-bromo-2-deoxyuridine (BrdU) injection intravenously 1 day before killing. Tissue sections of tongues were stained with anti-BrdU antibody to evaluate numbers of replicating cells. Haematoxylin and eosin plus trichrome staining were performed to assess muscular structure.

Results: Reduction tongues contained significantly more BrdU+ cells compared to sham tongues ($P < 0.01$). However, these BrdU+ cells were mostly identified in reparative connective tissues (fibroblasts) rather than in regenerating muscle tissue (myoblasts). Trichrome-stained sections showed disorganized collagen fibres linked to few intermittent muscle fibres in the reduction tongues. These myofibres presented signs of atrophy with reduced perimysium and endomysium. Matrix between reduced perimysium and endomysium was filled with fibrous tissue.

Conclusions: Fibrosis without predominant myogenic regeneration was the major histological consequence of surgical tongue volume reduction.

Correspondence: Z. J. Liu, Department of Orthodontics, University of Washington, Box 357446, Seattle, WA 98195, USA. Tel.: (206)616-3870; Fax: (206)685-8163; E-mail: zjliu@u.washington.edu

Introduction

The tongue plays an important role in various oral functions such as respiration, speech, deglutition and mastication. As a large muscular organ comprised of four intrinsic (superior longitudinal, inferior longitudinal, transversus and verticalis) and four extrinsic (genioglossus, styloglossus, palatoglossus and hyoglossus) muscles, the tongue fills the majority of the oral cavity in most mammals. Previous studies have demonstrated that alteration of tongue volume significantly affects functional loads on its surrounding osseous tissues (1), thus resulting in profound effects on craniofacial growth and occlusal development, over time (2).

In addition to its application in different types of true macroglossia (3–6), surgical tongue volume reduction is a relatively common part of adjunct treatment for Class III skeletal malocclusion (prognathism), severe open bite and bimaxillary dento-alveolar protrusion (7,8), such as mandibular setback and maxillary *Le Fort* osteotomy, in order to adapt space-reduced oral cavity, lower risk of relapse and obtain better overall function. However, little has been identified regarding healing processes and morphological/histological consequences in the tongue after such surgical procedures.

A number of studies has shown that skeletal muscle is capable of extensive and prompt regeneration after injury, and the healing process occurs through destruction, repair and remodelling phases (9–13). Regeneration of myofibres begins with activation of myogenic precursors, the satellite cells. These quiescent cells are normally located between the basal lamina and plasma membrane of myofibres, and are activated by disruption of the sarcolemma and consequent myofibre necrosis. They proliferate and differentiate as myoblasts that fuse to form multinucleate myotubes, which may subsequently fuse with surviving

stump myofibres, thus providing continuity across the injured region (14–16). Newly formed myotubes produce muscle-specific proteins and mature into conventionally recognizable muscle fibres with peripherally located nuclei (10,16–20). Also during the repair phase, fibroblasts invade the damaged area and begin to produce extracellular matrix (ECM) to restore framework of the connective tissue (21,22). In most situations, severely destroyed muscle fibres are replaced by fast growing fibrous tissue, which compromises function of the affected muscles (23). It has also been demonstrated that populations of muscle precursor cells (MPC) within craniofacial muscles are distinct from certain types of skeletal muscle, such as limb muscles. Craniofacial muscles regenerate less effectively than limb muscle in response to both exogenous and endogenous injuries (24).

Muscle healing after surgical injury is a complex process requiring coordinated interaction between MPCs or satellite cells, growth factors, cytokines, inflammatory components, vascular components and ECM (25). To date, there has been no effective therapeutic approach to improve muscle healing. While glossectomy is applied extensively clinically, very few studies have been carried out to examine its healing and repair processes either in clinical or laboratory settings. The present study has been performed to address this topic and to test the hypothesis that partial fibrosis without predominant myogenic regeneration is the major histological consequence after surgical tongue volume reduction.

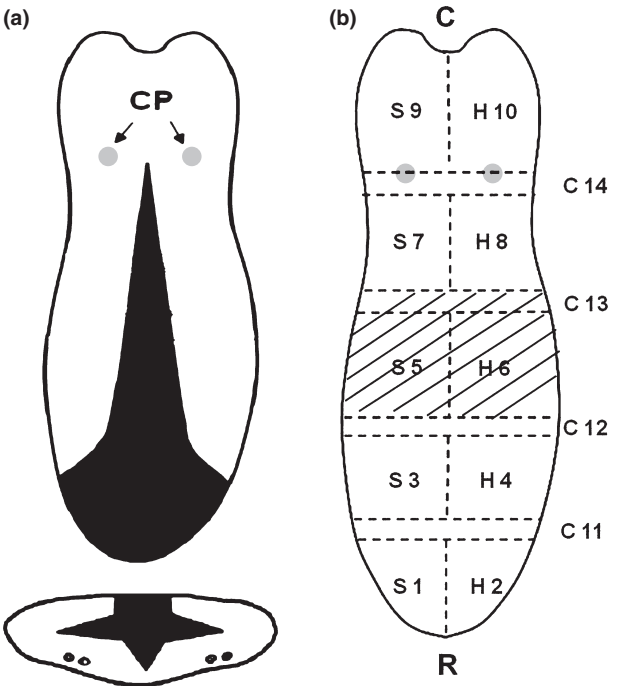

Figure 1. Schema of tongue volume reduction surgery and demarcation of histological sections. (a) Surgical incision lines in dorsal and cross-sectional views. Black portions of diagram depict the removed tongue tissue. CP, circumvallate papilla. Dots indicate the location of the neurovascular bundles in the ventral area of the tongue. (b) Schematic of locations for histological sections from three directions of the tongue. R, Rostral; c, Caudal; S, sagittal sectioning; C, coronal sectioning; H, horizontal sectioning. The hatched section is the central part of surgery-involving area which was used for anti-BrdU staining.

Materials and methods

Tongue surgery

Five sibling pairs (three males and two females) of 12-week-old Yucatan minipigs were obtained from Sinclair Research Center, MO. Of each pair, one was subjected to midline uniform glossectomy (reduction) as clinically performed (3) (Fig. 1a), and the other underwent sham surgery. Tongue tissue was removed uniformly in three dimensions by 15–18% of its original volume (26). Sham surgery was performed by making an incision 2–3 mm deep from the tongue surface with the same pattern as used for tongue reduction surgery, but without tissue removal. Animals were maintained for 4 weeks after surgery. Body weights were monitored twice weekly over the experimental period. All procedures were approved by the University of Washington Institutional Animal Care and Use Committee.

Specimen preparation

One day before killing, 5-bromo-2-deoxyuridine (BrdU) was injected (40 mg⁄kg) into the pigs through the left ear vein. BrdU labels cells undergoing DNA replication in S phase of the cell cycle. Thus, postmortem quantification of BrdU-labelled cells provides a direct measurement of cell proliferation and progeny differentiation can be observed in tongues after reduction or sham surgery. Upon killing, cardiac perfusion was performed with 0.9% saline solution followed by diluted Prefer, a formalin-free fixative (Anatech Ltd, Battle Creek, MI, USA), then tongues were harvested. After fixations for 1.5–2 weeks in Prefer solution, excised tongues were divided into 14 and 11 (without blocks S1, H2 and C11) blocks for sham and reduction tongues, respectively (Fig. 1b). These blocks provided composite three directional view of tongue structures, that is, sagittal (S1, 3, 5, 7, 9), horizontal (H2, 4, 6, 8, 10) and coronal (C11, 12, 13 14) in three anatomical zones of the tongue, blade, body and base (26). All blocks were embedded in paraffin wax, sectioned at thickness of 10 μm, and stained with either haematoxylin & eosin (H&E) or Masson's trichrome. Numbers and orientations of myofibre bundles, distribution and size of individual muscle fibres, and perimysium and

endomysium of myofibres in each direction, were examined. Distribution and organization patterns of collagen fibres and their relationships to myofibre bundles were also evaluated. Serial sections from blocks S5 (sagittal), H6 (horizontal) and C13 (coronal), centre regions of surgery-involved areas (Fig. 1b, hatched area), were stained for BrdU-labelled cells to examine cell proliferation activity using the slightly modified protocol, previously used on rats (27). Briefly, staining procedures were as follows: tissue sections were incubated sequentially at room temperature with (i) primary antibody to BrdU-labelled DNA [diluted 1:150 in phosphate-buffered saline (PBS)] for 60 min; (ii) secondary antibody (biotinylated horse antimouse IgG) for 30 min, (iii) tertiary antibody (streptavidin horseradish peroxidase) for 30 min and (iv) 3,3′-diaminobenzidine (DAB) for 90 s. Sections were washed in PBS (5 min, three times) after each step.

Image capture and data processing

Low magnification (1×) images showing the entire section were first captured using a Nikon Eclipse E400 microscope (Nikon Corporation, Tokyo, Japan) and MetaVue software (Universal Imaging Co., Downtown, PA, USA). Each 1× sagittal or coronal images was further divided into nine subregions, and each 1× horizontal image was divided into six subregions (Fig. 2a–c). One 4× image was saved for general assessment of each selected subregion at each direction, and two 40× images were further captured separately from central-top and central-bottom portions of each 4× image (Fig. 2d).

To collectively demonstrate regional distribution of BrdU+ cells in three directions, counted cells from particular subregions were further grouped according to orientation. For sagittal sections, groups were vertical (dorsal, centre and ventral) and longitudinal (rostral, middle and

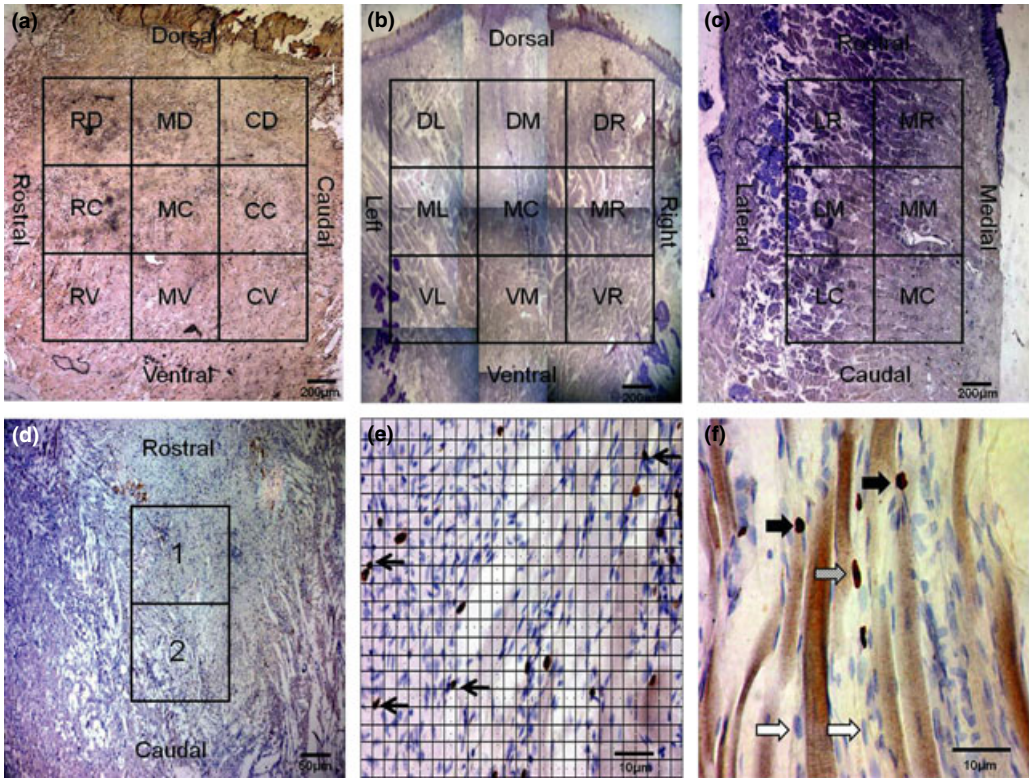

Figure 2. Regional assignment for cell counting and illustrations of cell counting and cell types. (a) 1× image of sagittal section, which was divided into nine subregions: rostral dorsal (RD), middle dorsal (MD), caudal dorsal (CD), rostral centre (RC), middle centre (MC), caudal centre (CC), rostral ventral (RV), middle ventral (MV) and caudal ventral (CV). (b) 1× image of coronal section, which was also divided into nine subregions: dorsal right (DR), dorsal middle (DM), dorsal left (DL), middle right (MR), MC, middle left (ML), ventral right (VR), ventral middle (VM) and ventral left (VL). (c) 1× image of horizontal section, which was further divided into six subregions: medial rostral (MR), medial middle (MM), medial caudal (MC), lateral rostral (LR), lateral middle (LM) and lateral caudal (LC). (d) 4× image showing two sampling fields (1, central-top; 2, central-bottom) in each subregions above. (e) 40× image showing the methods for BrdU+ cells counts (arrows) using a calibrated grid. (f) 60× image showing different cell types. BrdU+ fibroblast nuclei (stripped arrows); BrdU+ myofibre nuclei (solid arrows); BrdU− cells (empty arrows).

caudal) (Fig. 2a). For coronal sections, groups were vertical (dorsal, centre and ventral) and transverse (left, centre and right) (Fig. 2b). Longitudinal (medial and lateral) and transverse (rostral, middle and caudal) groups were applied for horizontal sections (Fig. 2c).

MetaMorph software (Universal Imaging Co.) was used for total BrdU+ cell counting, which allowed user-configurable measurement grids for images, and measurement was carried out within each element in the grid. Grids composed of 27 vertical and 20 horizontal lines were applied for these cell counts, which produced 115 mm^2 fields and 588 square boxes with dimensions of 14 μm for each box and 567 intersections. Only BrdU+ cells touching intersections of the grid were counted, and numbers from the two 40× images were averaged for each subregion (Fig. 2e).

Morphology of BrdU+ cells was identified to be mostly round to elliptical with dark-brown stained nuclei (Fig. 2f, solid and striped arrows). Counting was limited to muscular tissues and did not include epithelium because of its very active nature of cell replication over lifetime. While satellite cells and/or myoblasts could not be distinguished without application of double staining for sarcolemmal or myoproteins such as desmin, tropomyosin and skeletal actin, attention was paid to distinguish BrdU+ myogenic cells (satellite cells and/or myoblasts) from BrdU+ connective tissue cells (fibroblasts) in each direction according to cell shapes and locations. Myogenic cells were only identified when BrdU+ nuclei were located outside the sarcolemma but inside the basal lamina (28–31), that is, only nuclei associated with myofibre were denoted as myonuclei, which included satellite cells and/or myoblasts (Fig. 2f). In addition to location, cell morphology was considered as a further identifier. Myonuclei were mostly round in shape, whereas fibroblast and endothelial nuclei were found elsewhere as elliptical to spindle-shaped (Fig. 2f). Adipose cell nuclei were identified as non-centrally located nuclei (in white adipose cells) and round centrally located nuclei (in brown adipose cells). These adipose cells were also excluded from the present assessment. Because of limited appearance, myonuclear BrdU+ cells were counted without using intersections of the grid as described earlier. Thus, in a given image, BrdU+ connective tissue cells were only counted when they appeared at intersections of the grid, whereas BrdU+ myonuclei cells were counted without this restriction.

To test reproducibility, recounting was performed for 10 randomly selected images, and these counts were then compared to original counts using Dahlberg's equation ($\sqrt{\sum d^2/2n}$) (32). In this equation, d is the overall difference in two separate counts of selected samples and n is the number of samples; errors for total BrdU+ and BrdU+ myonuclear counts were 0.24 and 0.15 respectively.

Haematoxylin & eosin and trichrome images from the different orientations were also captured using the same equipment as for BrdU+ cell counting under the different magnifications, which were used for evaluating overall muscular structure of the tongue qualitatively.

Statistical analysis

Descriptive data were first examined for distribution using SPSS® statistical package (ver. 11.0; SPSS Inc, Chicago, IL, USA), and parametric statistical approaches were applied as the data were of normal distribution. Independent *t*-tests were used to detect differences between sham operated and reduction tongues for the same subregions or grouped regions, and one-way ANOVA, followed by Tukey *post hoc* tests were applied for comparing differences of regions in each group. Significance level was set at $P < 0.05$.

Results

Assessment of overall cell proliferation

Myogenic and connective tissue BrdU+ cells were found in both reduction and sham tongues, but their overall appearances were relatively fewer cells in sham than in reduction tongues. Myonuclei were only found in newly formed myofibres, however, fibroblast nuclei were found elsewhere in the matrix between perimysium and endomysium (Fig. 2f). Overall ratios of BrdU+ myonuclei to BrdU+ connective tissue nuclei were about 1–1.2 in sham operated tongues and 0.6–0.7 in the reduction tongues respectively.

Subregions aligning in the same orientation in each direction were grouped to present regional differences of cell proliferation activity between reduction and sham tongues. Thus, there were vertical regions in both sagittal and coronal sections (dorsal, middle and ventral), and longitudinal regions in both sagittal and horizontal sections (caudal, middle and rostral), and transverse regions in both coronal (left, middle and right) and horizontal (medial and lateral) sections. Cell counting in vertical regions of coronal sections and transverse regions of horizontal sections was not performed as these numbers were obtained from counts of sagittal and coronal sections (Fig. 2a–c).

Overall, counts of BrdU+ cells in all three directions were significantly higher in the reduction over sham tongues in almost all grouped regions ($P < 0.01$) (Fig. 3). In sagittal sections of reduction tongues, highest and lowest counts were found to be in caudal central (CC) and caudal dorsal subregions respectively. In sham tongues, however, highest counts were found in the rostra-dorsal subregion, while lowest were found in the CC among all subregions

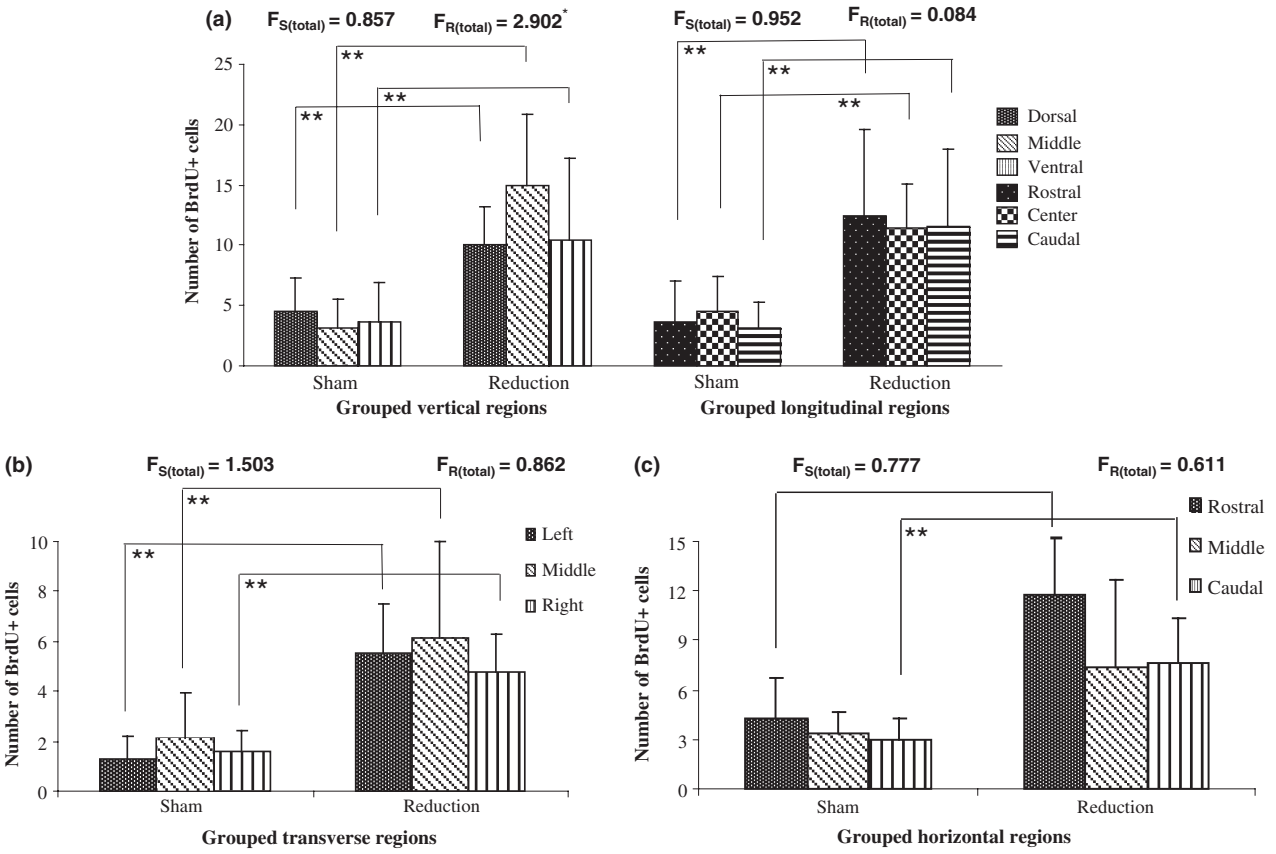

Figure 3. Comparisons of the total BrdU+ cells for grouped regions between the reduction and sham tongues. (a) sagittal sections, showing the cell populations in the grouped vertical and longitudinal regions; (b) coronal sections, showing the cell populations in the grouped transverse region; (c) horizontal sections, showing the cell populations in the grouped horizontal region. *$P < 0.05$; **$P < 0.01$.

of sagittal sections (Fig. 3a). Grouped vertical regions further showed a pyramidal effect, in which centres of the regions contained significantly higher numbers of proliferating cells ($P < 0.01$, Fig. 3a). Dorsal and ventral regions had similar amounts of proliferating activity. Longitudinally, highest counts were seen in the rostral region, while middle and caudal regions had slightly fewer BrdU+ cells. In comparison to vertical grouped regions of reduction tongues, dorsal regions of sham tongues presented highest counts followed by ventral and central regions. In the longitudinal grouped regions, sham tongues had the highest activity in middle zones followed by rostra-caudal regions (Fig. 3a).

Similar trends were also found in total counts of coronal sections, of which reduction tongues had significantly higher counts compared to those of shams in all three grouped regions ($P < 0.01$, Fig. 3b), and highest numbers were seen at middle centre, whereas the lowest were observed in middle ventral subregions of reduction tongues. Grouped transverse centre (middle) region exhibited larger counts than those of left and right regions (Fig. 3b). In sham tongues, however, cell proliferation activity had similar trends across the three grouped transverse regions with significantly lower cell numbers ($P < 0.01$, Fig. 3b).

Similarly, total BrdU+ cells were significantly higher in reduction tongues than shams in grouped longitudinal regions of horizontal sections ($P < 0.01$). While numbers of counted cells gradually decreased rostro-caudally in sham tongues, rostral regions had significantly higher cell numbers than middle and caudal regions in reduction tongues (Fig. 3c).

Assessment of myogenic cell proliferation

In sagittal and coronal sections, numbers of myoblasts were higher in reduction than in sham tongues in grouped vertical and transverse regions ($P < 0.01$), but numbers in grouped longitudinal regions were conversely smaller reduction than in sham tongues ($P < 0.05$–0.01) (Fig. 4a,b). There was no significant difference between numbers in reduction and sham tongues in grouped longitudinal regions of horizontal sections (Fig. 4c). Regional

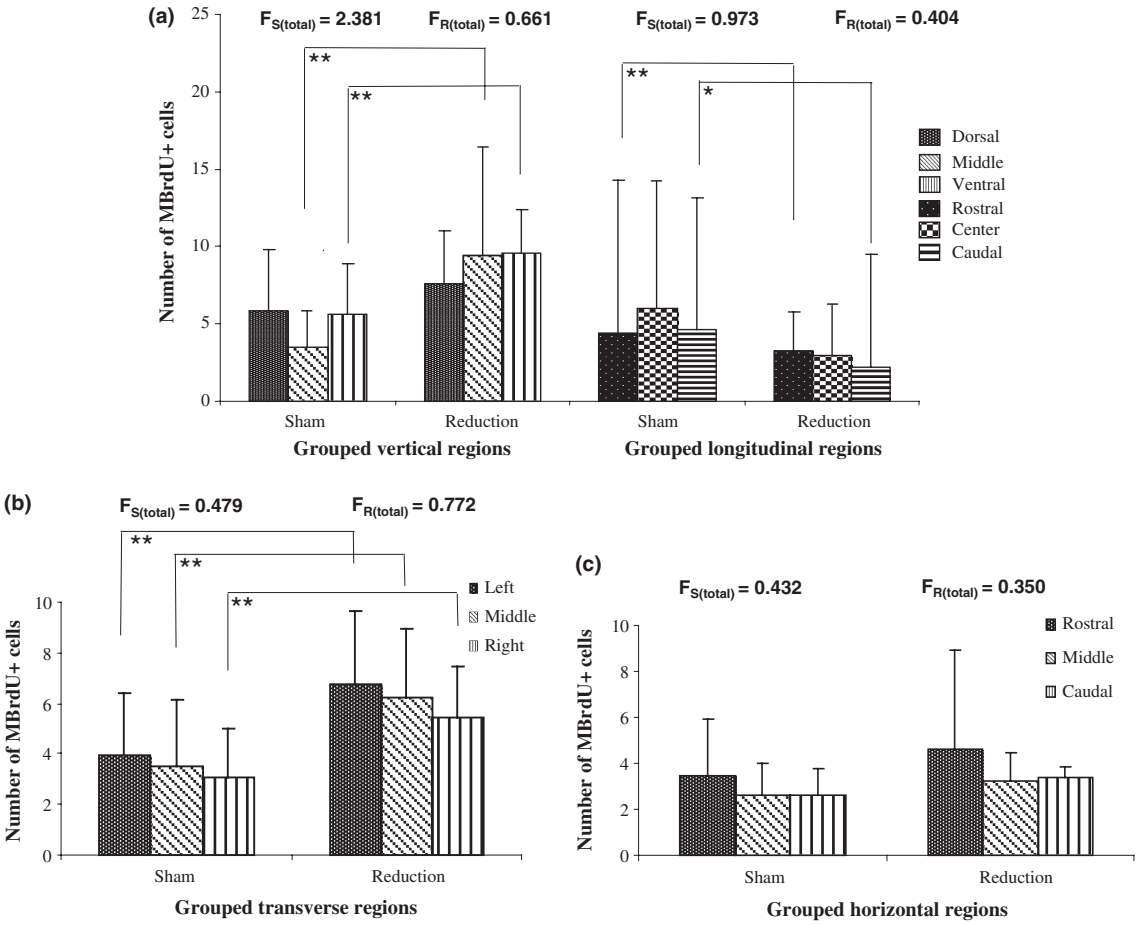

Figure 4. Comparisons of BrdU+ myonuclei (MBrdU+) cells for grouped regions between the reduction and sham tongues. (a) sagittal sections, showing the cell populations in the grouped vertical and longitudinal regions; (b) coronal sections, showing the cell populations in the grouped transverse region; (c) horizontal sections, showing the cell populations in the grouped horizontal region. *$P < 0.05$; **$P < 0.01$.

differences of BrdU+ myonuclear cell counts showed less clear trends than overall BrdU+ cell counts.

Assessment of muscular structure

Tongue architecture in surgical areas was almost totally taken with newly regenerated fibrous connective tissue in centripetal patterns, and muscle regeneration processes also followed a typical centripetal gradient (Fig. 5a). Remaining intermeshed myofibres could be seen in surrounding non-surgery areas (Fig. 5b).

In coronal sections of sham tongues, vertical muscle fibres were observed as bundles that ran obliquely from ventral to dorsal sides. This type of structure was seen more in dorsal halves of the tongue. Longitudinal muscle was transected, and transverse and vertical muscle fibres intertwined with each other as they ran within bundles of longitudinal muscle (Fig. 6a). In reduction tongues, despite the oblique characteristic, some vertical fibres running from lamina propria, were aligned strictly vertically by crossing transverse fibres, in which numbers of parallel fibres were seen, without mutual interweaving (Fig. 6b).

In sagittal sections of sham tongues, transverse and vertically running myofibres were seen to be transected at different angles, where the muscle bundles could be visualized; longitudinal muscle fibres ran parallel in anteroposterior direction (Fig. 6c). In reduction tongues, not only transversely running myofibres were totally transected, but also vertically running myofibres were transected at different angles (Fig. 6d). Fibroblast proliferation was found in the matrix of dorsal middle (DM) areas of reduction tongues (Fig. 6e), between perimysium and endomysium.

In horizontal sections of sham tongues, collagen and myofibres were found in a well-organized arrangement, and collagen-rich underlying lamina propria and multiple transverse muscle fibre bundles were interwoven with many vertical plus few longitudinal fibres (Fig. 7a). These

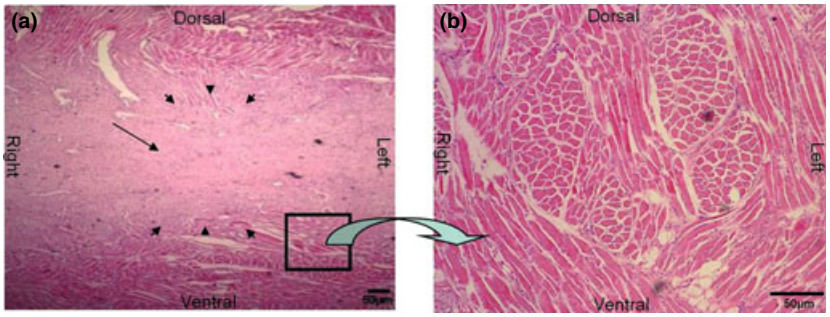

Figure 5. Pattern of muscle repair after the surgery (H&E staining). (a) a 4× coronal image from a reduction tongue, showing the scar tissue in the middle centre area (MC); the centripetal repair was shown by small arrows. (b) a 10× coronal image from the insert area of the image (a), showing a number of intermeshed myofibres surrounding the scar tissue.

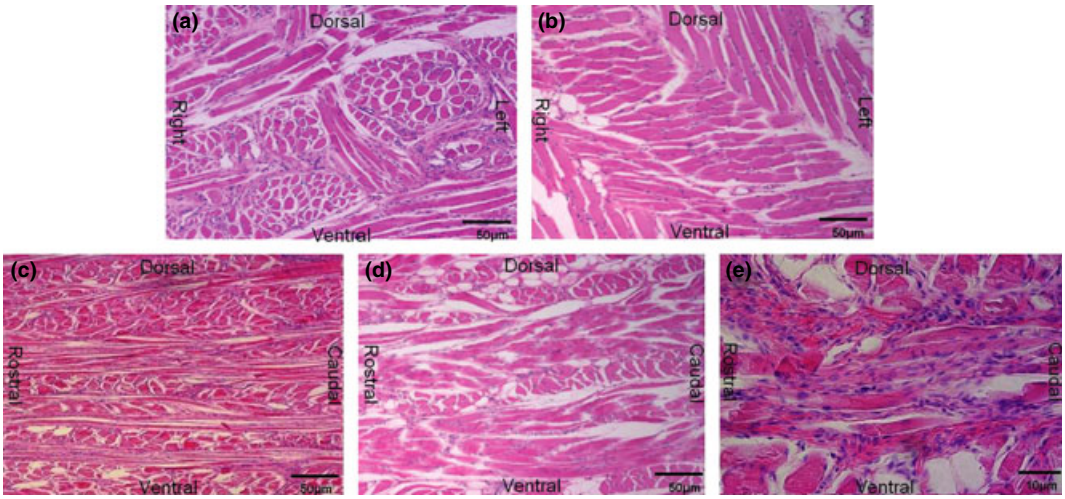

Figure 6. Muscular structures in the sham and reduction tongues (H&E staining). (a) a 10× coronal image from a sham tongue. (b) a 10× coronal image from a reduction tongue. (c) a 10× sagittal image from a sham tongue. (d) a 10× sagittal image from a reduction tongue. (e) a 40× sagittal image from a reduction tongue.

collagen fibres were localized and also organized in bundles. Disorganized collagen fibres linked with few intermittent muscle fibres were seen in reduction tongues (Fig. 7b, inset).

Overall, myofibre reconstitution had disorganized arrangement in all sagittal, horizontal and coronal sections in reduction tongues compared to sham tongues (compare Fig. 7a,b). Trichrome staining of sagittal sections further highlighted collagen-rich areas near incision sites, which had significantly higher percentages of fibroblast proliferation and lower percentage of myofibres than sham tongues. Long axis diameters of centronucleate myofibres were much smaller than those in sham tongues, a sign of atrophy, with reduced perimysium and endomysium. In addition, the amount of connective tissues was significantly higher compared to sham tongues (compare Fig. 7c,d). However, myofibres reduced in number and size could still easily be found at surgical sites of reduction tongues. Despite the lack of muscle reconstitution, trichrome staining showed sporadic strands of myofibres within the network of collagen (Fig. 7d).

Discussion

Cell proliferation and myogenic regeneration of the surgically injured tongues were comprehensively evaluated from sagittal, horizontal and coronal orientations in the present study. In the sagittal view of reduction tongues, myoblasts were scattered around connective tissue and within bundles of muscle fibres, which were disconnected from other muscle fibres and randomly located within a section. The majority of cell activity shown in tissue sections, however, was proliferation of connective tissue cells, which were randomly oriented and extended into underlying striated muscles. Given that less myofibre nuclei were identified in sagittal central necrotic zones,

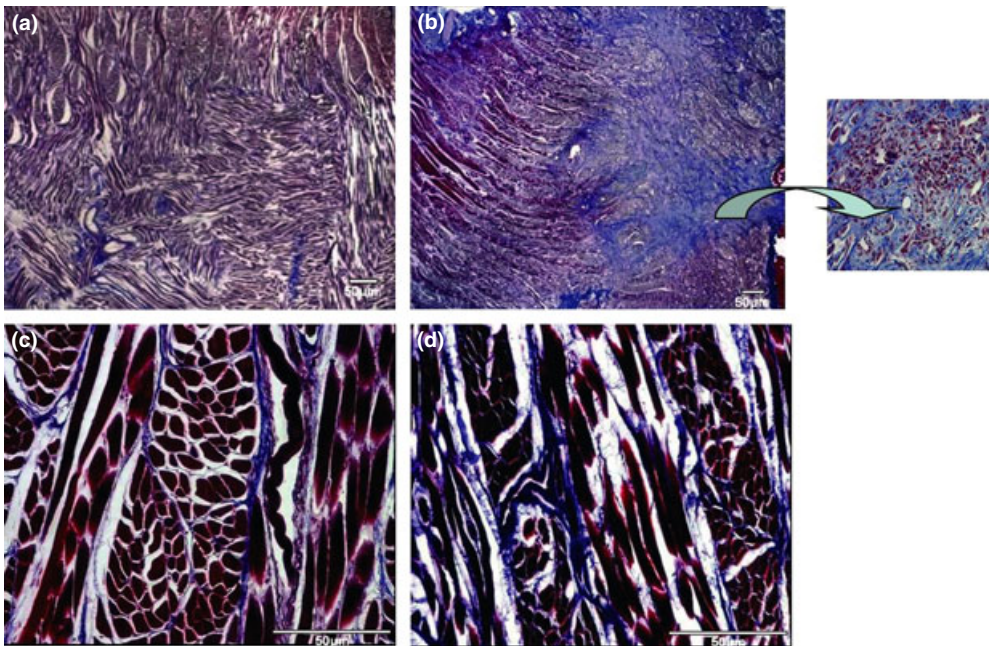

Figure 7. Muscular structures in the sham and reduction tongues (trichrome staining). (a and b) 4× horizontal images showing muscular structure from sham (a) and reduction (b) tongues. Note that the collagen fibres and myofibres alignment are arranged in a well-organized fashion in the sham tongue. However, the amounts of connective tissues are significantly higher in the reduction tongue compared with the sham tongue. The insert area of image (b) shows disorganized collagen fibres linked with a few intermittent muscle fibres. (c and d) 20× sagittal images showing the endomysium and perimysium from sham (c) and reduction (d) tongues. Note that myofibres (red) present atrophy with the reduced endomysium and perimysium, and fibrous tissues (blue) are fully interposed between the atrophied myofibres.

better resistance of satellite cells at the periphery must account for centripetal progress of regeneration. Besides that, reduction tongues also showed that cell proliferation in these connective tissues was much less organized and was scattered randomly compared to sham tongues. In the coronal view of reduction tongues, mid regions had highest BrdU+ total cell counts, which was due to fibrotic scar tissue deposition, located near the incision where main cell activity resided. BrdU+ myofibre nuclei were also seen within connective tissue areas where fibres were randomly disconnected. In the horizontal view, connective tissue cells near the incision had lower proliferative activity in sham rather than reduction tongues. Most importantly, there were quantitative differences between labelled myofibre nuclei and connective tissue cell nuclei with higher proliferative activity in reduction over sham tongues, although patterns were similar to each other.

In all views, of the three orientations, sham tongues had more BrdU+ myonuclei compared to BrdU+ connective tissue cell nuclei. In contrast, reduction tongues had the opposite trend, that is, more BrdU+ connective tissue cell nuclei and less BrdU+ myonuclei. This finding clearly indicates that proliferation of connective tissue cells prevailed, while capacity of myogenic regeneration was limited in reduction tongues. On the other hand, despite higher proliferative activity of BrdU+ myofibre nuclei in sham tongues, absolute counts of total BrdU+ nuclei were still lower in shams than in reduction tongues. Thus, enhanced cell proliferative activity in reduction tongues was not attributable to active myogenic regeneration in response to surgery, but was scar tissue formation or fibrosis presented by active cell proliferation in connective tissue cells and vascular endothelium. The present study also revealed that the sagittal view usually produced higher counts of BrdU+ cells in comparison to coronal and horizontal sections. This difference may be accounted for as muscle fibres and connective tissues of the tongue are oriented more longitudinally than transversely and/or in dorso-ventral directions.

Muscle repair processes are characterized by a degeneration phase followed by regeneration phase in a time-dependent manner. The initial event is muscle degeneration and inflammation, which occurs within the first minutes of injury and continues for up to 1–2 weeks after. Muscle regeneration becomes apparent starting at 2 days after muscle fibre damage, especially in the obvious increase in MPCs; by 4 or 5 days post-injury, muscle fibres are almost completely established, and after that, fibres grow and elongate further without forming new fibres (33). Similar time courses would be expected in tongue striated

muscle. Fibrosis usually occurs at 2 weeks after injury and increases over time for up to 4 weeks post-injury (25). It should be noted that pigs in the present study were maintained for 4 weeks after surgery and BrdU was injected 1 day prior to killing. This could probably be the reason why connective tissue prevailed, especially in reduction tongues at the end point.

An experimental consideration for repair of tongue is the observation of its centripetal pattern. This pattern follows a gradient that flows from outer to inner regions, resulting in formation of different zones within regenerating myofibres (25). The outer region is considered to contain most mature myofibres, while inner regions contain less mature ones. Studies have shown that the diameter of regenerating myofibres increases following a centripetal gradient up to day 14. By day 28, all regenerated myofibres are centronucleate and their polygonal shape and organization in fascicles are close to those of normal myofibres (34). This type of myogenic regeneration was also found in the present study, based on the cell assessment of different regions in sagittal sections. In reduction tongues, the central region had highest proliferative activity, whereas that of dorsal and ventral regions was relatively low. Thus, the higher proliferation in the centre region compared to dorsal region showed episodes of the healing process, which occurred first in the dorsal region and later in the central region, indicating a clear sign of the centripetal pattern of the repair, as seen in other injured muscles (34). The ventral region had the lowest proliferative activity, lower than central and dorsal regions, because it was less involved by midline uniform tongue reduction surgery, which intended to conserve neurovascular bundles located in ventral regions of the tongue.

Myoarchitecture of the tongue is believed to consist of a complex network of interwoven fibres and fibre bundles. Because of the location of the incision here, extrinsic muscles were less affected, thus the repair process occurred mainly in intrinsic tongue muscles. These muscles are organized in three different directions and with distinct fascicular layers or small bundles of fibres interdigitating with each other at approximate right angles. Based on three directional views of the surgical area, muscular fibres running in longitudinal, transverse and vertical orientations were all transected by the surgical incisions from different angles, and reconstructed muscle structure was more organized in sham than in reduction tongues, implying that complete functional recovery from surgery in reduction tongues might not be possible because the reconstitution of the muscular structures was not accomplished.

Myogenic regeneration is a complex process during which both extrinsic and intrinsic factors play important roles. Factors that control and alter this process include satellite cell activation, migration to the injury site, proliferation of MPCs and differentiation to myotubes and myofibres (25). Alternatively, fibroblasts invaded the gap and began to produce ECM to restore the framework of the structures, and fibrosis occurred leading to the formation of scar tissue. Compared with the sham tongues, the surgical area in the reduction tongues was mostly composed of collagen-rich fibre bundles, a sign of partial fibrosis. When fibrotic tissues form the surgical area, the recovery of normal tissue architecture and functionality are compromised. Fibrosis may cause decreased muscle contractility and reduction in the range of movement. Furthermore, excessive fibroblast proliferation produced a larger scar that may limit the extent of myogenic regeneration. These consequences could cause the functional recovery of tongue musculature remaining incomplete. Therefore, the healing or repair of the injured tongue is not the reconstitution of muscle fibres but an adaptation to a new morphology after surgical injury.

There are two possibilities of myogenic fate following surgical tongue volume reduction. Myofibres that were found within the scar tissue might originate from the sprout of residual myofibres and they were actually regenerating ones from myonenic progenitor cells, i.e. satellite cells. As stated previously, because the double staining for the sarcolemmal label was not applied, the present study lacks of power to identify the source of origin for BrdU+ cells. Nevertheless, given the fact that the majority of BrdU+ myonuclei cells were found in the disconnected muscle fibres near the surgical sites, it is reasonable to assume that these cells originated from the myogenic progenitor pool located between the basal lamina and plasma membrane of the tongue (35). Furthermore, as the myogenic regeneration was centripetal by progressing from the outer to inner regions, the formation of successive zones of degeneration and regeneration was visualized in the present study. Because of the limited time period, the present study might lack the capacity to reveal the fate of these regenerated myofibres and to know whether they eventually fuse to rebuild the tongue muscular structure. However, it has been demonstrated that when the formation of scar tissue (fibrosis) begins between the second and third weeks after injury, and increases in size over time, this appears to be the end product of the muscle regeneration process (11). We therefore believe that as long as the scar is formed and exists in the reduction tongues, a complete reconstruction of muscular structure and fully functional recovery are unlikely to occur.

Muscle healing and repair involves myogenesis, reinnervation and revascularization, and this process is regulated by multiple biochemical and molecular pathways, including those initiated by inflammatory cytokines, growth factors and the evolutionarily conserved Notch,

Wnt and Sonic Hedgehog signalling pathways (36–39). It also has been shown that the growth factors, including insulin-like growth factor-1, basic-fibroblast growth factor and nerve growth factor, can improve muscle regeneration during the preliminary phase of healing, but the post-injury healing process remains incomplete (11,40,41). Fibrosis, on the other hand, is demonstrated by large increases in collagens types I and III in muscle ECM. Fibrosis is regulated by signalling through transforming growth factor-β (TGF-β) and offset by upstream hepatocyte growth factor signalling, which acts as a TGF-β antagonist (42). However, none of the growth factors that have been investigated appears capable of completely healing the injured muscle, possibly because of the development of fibrosis. The use of anti-fibrosis agents that antagonize the effect of TGF-β can prevent fibrosis and improve muscle healing and repair, resulting in nearly complete recovery (11). Optimal muscle recovery may require the use of novel technologies, such as gene therapy and tissue engineering, to achieve both high levels and long-term persistence of these growth factors and cytokines within the injured muscle.

Therefore, the development of biological approaches to prevent muscle from fibrosis should have a great potential to enhance muscle healing and repair. However, if the scar already forms as seen in the present study, the approaches must require the elimination of the scar tissue prior to the application for enhancement of myogenic regeneration and the prevention of ECM deposition. To date, biological approaches to improve muscle healing by enhancing myogenic regeneration and reducing the formation of fibrosis remain to be investigated and developed.

In conclusion, from the present study, we suggest that (i) myogenic regeneration of the surgically injured tongue follows a centripetal pattern and was complete in sham but incomplete in reduction tongues after surgery, (ii) partial fibrosis without predominant myogenic regeneration was the major histological consequence in reduction tongues after surgery, (iii) because the repair was not reconstitution of muscular structure but was an adaption to new morphology, the intricate three-dimensional architecture of tongue musculature was not reconstructed and (iv) excessive fibrosis and formation of scar in the surgical area hindered the process of myogenic regeneration, which in turn limited functional recovery of the tongue after surgery.

Acknowledgements

The authors would like to thank Dr. Susan Herring for her constructive discussions and critical comments and Dr. Yinzhong Duan for his full support on this project. Thanks also goes to Drs. Volodymyr Shcherbatyy and Xian-Qin Bai for their help on animal experiments, histology, and general lab assistance. This study was supported by the grant R01DE15659 and T32DE007132 from NIDCR to ZJL and ZJL/AFA. The participation of WMY was supported by China Government Scholarship (File No 2008659018).

References

1 Liu ZJ, Shcherbatyy V, Perkins JA (2008b) Functional loads of the tongue and consequences of volume reduction. *J. Oral Maxillofac. Surg.* **66**, 1351–1361.
2 Liu ZJ, Shcherbatyy V, Gu G, Perkins JA (2008a) Effects of tongue volume reduction on craniofacial growth: a longitudinal study on orofacial skeletons and dental arches. *Arch. Oral Biol.* **53**, 991–1001.
3 Davalbhakta A, Lamberty BG (2000) Technique for uniform reduction of macroglossia. *Br. J. Plast. Surg.* **53**, 294–297.
4 Gasparini G, Saltarel A, Carboni A, Maggiulli F, Becelli R (2002) Surgical management of macroglossia: discussion of 7 cases. *Oral Surg. Oral Med. Oral Pathol. Oral Radiol. Endod.* **94**, 566–571.
5 Herren P, Muller-Boschung P, Stutz G (1981) Macroglossia and partial resection of the tongue out of orthodontic indication. *Proc. Finn. Dent. Soc.* **77**, 45–55.
6 Wolford LM, Cottrell DA (1996) Diagnosis of macroglossia and indications for reduction glossectomy. *Am. J. Orthod. Dentofacial Orthop.* **110**, 170–177.
7 Deguchi T (1993) Case report: three typical cases of glossectomy. *Angle Orthod.* **63**, 199–207.
8 Ruff RM (1985) Orthodontic treatment and tongue surgery in a class III open-bite malocclusion. A case report. *Angle Orthod.* **55**, 155–166.
9 Allbrook D (1981) Skeletal muscle regeneration. *Muscle Nerve* **4**, 234–245.
10 Carlson BM, Faulkner JA (1983) The regeneration of skeletal muscle fibers following injury: a review. *Med. Sci. Sports Exerc.* **15**, 187–198.
11 Huard J, Li Y, Fu FH (2002) Muscle injuries and repair: current trends in research. *J. Bone Joint Surg. Am.* **84-A**, 822–832.
12 Jarvinen M, Aho AJ, Lehto M, Toivonen H (1983) Age dependent repair of muscle rupture. A histological and microangiographical study in rats. *Acta Orthop. Scand.* **54**, 64–74.
13 Menetrey J, Kasemkijwattana C, Day CS, Bosch P, Vogt M, Fu FH *et al.* (2000) Growth factors improve muscle healing in vivo. *J. Bone Joint Surg. Br.* **82**, 131–137.
14 Bischoff R (1994) The satellite cell and muscle regeneration. In Engelbert RH, Franzini-Armstrong C ed. *Myology*, 2nd edn, pp. 97–119. New York: McGraw-Hill Inc..
15 Hurme T, Kalimo H (1992) Activation of myogenic precursor cells after muscle injury. *Med. Sci. Sports Exerc.* **24**, 197–205.
16 Schmalbruch H (1976b) Skeletal muscle regeneration. *Verh. Anat. Ges.* **70**, 691–701.
17 Carpenter S, Karpati G (2001) *Pathology of Skeletal Muscle*, pp. 28–129. New York: Oxford University Press Inc..
18 Grounds MD (1991) Towards understanding skeletal muscle regeneration. *Pathol. Res. Pract.* **187**, 1–22.
19 Roth D, Oron U (1985) Repair mechanisms involved in muscle regeneration following partial excision of the rat gastrocnemius muscle. *Exp. Cell Biol.* **53**, 107–114.
20 Schmalbruch H (1976a) The morphology of regeneration of skeletal muscles in the rat. *Tissue Cell* **8**, 673–692.
21 Hurme T, Kalimo H, Sandberg M, Lehto M, Vuorio E (1991) Localization of type I and III collagen and fibronectin production in injured gastrocnemius muscle. *Lab. Invest.* **64**, 76–84.

22 Lehto M, Duance VC, Restall D (1985) Collagen and fibronectin in a healing skeletal muscle injury. An immunohistological study of the effects of physical activity on the repair of injured gastrocnemius muscle in the rat. *J. Bone Joint Surg. Br.* **67**, 820–828.
23 Nikolaou PK, Macdonald BL, Glisson RR, Seaber AV, Garrett WE Jr (1987) Biomechanical and histological evaluation of muscle after controlled strain injury. *Am. J. Sports Med.* **15**, 9–14.
24 Pavlath GK, Thaloor D, Rando TA, Cheong M, English AW, Zheng B (1998) Heterogeneity among muscle precursor cells in adult skeletal muscles with differing regenerative capacities. *Dev. Dyn.* **212**, 495–508.
25 Charge SB, Rudnicki MA (2004) Cellular and molecular regulation of muscle regeneration. *Physiol. Rev.* **84**, 209–238.
26 Perkins JA, Shcherbatyy V, Liu ZJ (2008) Morphologic and histologic outcomes of tongue reduction surgery in an animal model. *Otolaryngol. Head Neck Surg.* **139**, 291–297.
27 Okafuji N, Liu ZJ, King GJ (2006) Assessment of cell proliferation during mandibular distraction osteogenesis in the maturing rat. *Am. J. Orthod. Dentofacial Orthop.* **130**, 612–621.
28 McLoon LK, Thorstenson KM, Solomon A, Lewis MP (2007) Myogenic precursor cells in craniofacial muscles. *Oral Dis.* **13**, 134–140.
29 Renault V, Rolland E, Thornell LE, Mouly V, Butler-Browne G (2002a) Distribution of satellite cells in the human vastus lateralis muscle during aging. *Exp. Gerontol.* **37**, 1513–1514.
30 Renault V, Thornell LE, Butler-Browne G, Mouly V (2002b) Human skeletal muscle satellite cells: aging, oxidative stress and the mitotic clock. *Exp. Gerontol.* **37**, 1229–1236.
31 Renault V, Thornell LE, Eriksson PO, Butler-Browne G, Mouly V (2002c) Regenerative potential of human skeletal muscle during aging. *Aging Cell* **1**, 132–139.
32 Dahlberg G (1940) *Statistical Method for Medical and Biological Students*. New York: Interscience Publications, pp. 33–40.
33 Grounds MD, Yablonka-Reuveni Z (1993) Molecular and cell biology of skeletal muscle regeneration. *Mol. Cell Biol. Hum. Dis. Ser.* **3**, 210–256.
34 Lefaucheur JP, Sebille A (1995) The cellular events of injured muscle regeneration depend on the nature of the injury. *Neuromuscul. Disord.* **5**, 501–509.
35 Mauro A (1961) Satellite cell of skeletal muscle fibers. *J. Biophys. Biochem. Cytol.* **9**, 493–495.
36 Conboy IM, Rando TA (2002) The regulation of Notch signaling controls satellite cell activation and cell fate determination in postnatal myogenesis. *Dev. Cell* **3**, 397–409.
37 Husmann I, Soulet L, Gautron J, Martelly I, Barritault D (1996) Growth factors in skeletal muscle regeneration. *Cytokine Growth Factor Rev.* **7**, 249–258.
38 Polesskaya A, Seale P, Rudnicki MA (2003) Wnt signaling induces the myogenic specification of resident CD45+ adult stem cells during muscle regeneration. *Cell* **113**, 841–852.
39 Wagers AJ, Conboy IM (2005) Cellular and molecular signatures of muscle regeneration: current concepts and controversies in adult myogenesis. *Cell* **122**, 659–667.
40 Jarvinen TA, Kaariainen M, Jarvinen M, Kalimo H (2000) Muscle strain injuries. *Curr. Opin. Rheumatol.* **12**, 155–161.
41 St Pierre Schneider B, Correia LA, Cannon JG (1999) Sex differences in leukocyte invasion in injured murine skeletal muscle. *Res. Nurs. Health* **22**, 243–250.
42 Huebner KD, Jassal DS, Halevy O, Pines M, Anderson JE (2008) Functional resolution of fibrosis in mdx mouse dystrophic heart and skeletal muscle by halofuginone. *Am. J. Physiol. Heart Circ. Physiol.* **294**, H1550–H1561.